Thermodynamic Analysis of Receptors Based on Guanidinium/Boronic Acid Groups for the Complexation of Carboxylates, α-Hydroxycarboxylates, and Diols: Driving Force for Binding and Cooperativity

Sheryl L. Wiskur, John J. Lavigne, Axel Metzger, Suzanne L. Tobey, Vincent Lynch, and Eric V. Anslyn*[a]

Abstract: The thermodynamics of guanidinium and boronic acid interactions with carboxylates, α-hydroxycarboxylates, and diols were studied by determination of the binding constants of a variety of different guests to four different hosts (**7**–**10**). Each host contains a different combination of guanidinium groups and boronic acids. The guests included molecules with carboxylate and/or diol moieties, such as citrate, tartrate, and fructose, among others. The Gibbs free energies of binding were determined by UV/Vis absorption spectroscopy, by use of indicator displacement assays. The receptor based on three guanidinium groups (**7**) was selective for the tricarboxylate guest. The receptors that incorporated boronic acids (**8**–**10**) had higher affinities for guests that included α-hydroxycarboxylate and catechol moieties over guests containing only carboxylates or alkanediols. Isothermal titration calorimetry revealed the enthalpic and entropic contributions to the Gibbs free energies of binding. The binding of citrate and tartrate was investigated with hosts **7**–**10**, for which all the binding events were exothermic, with positive entropy. Because of the selectivity of hosts **8**–**10**, a simple boronic acid (**14**) was also investigated and determined to be selective for α-hydroxycarboxylates and catechols over amino acids and alkanediols. Further, the cooperativity of **8** and **9** in binding tartrate was also investigated, revealing little or no cooperativity with **8**, but negative cooperativity with **9**. A linear entropy/enthalpy compensation relationship for all the hosts **7**–**10**, **14**, and the carboxylate-/diol-containing guests was also obtained. This relationship indicates that increasing enthalpy of binding is offset by similar losses in entropy for molecular recognition involving guanidinium and boronic acid groups.

Keywords: boronic acids · cooperativity · guanidinium groups · molecular recognition · thermodynamics

Introduction

One goal of supramolecular chemistry is the development of general design strategies for selective binding of a target molecule by a rationally designed synthetic receptor.[1] The targets often include biologically important guests such as saccharides,[2,3] natural products,[4] metals,[5] and ions.[6,7] Ultimately, the goal is to achieve selectivity and affinity comparable to those attained by natural receptors such as enzymes and antibodies. The selectivity and affinity of synthetic hosts is controlled and modulated by careful choice of a scaffold upon which binding moieties are appended, creating a binding pocket. A cleft with strong complementarity to the guest will improve selectivity,[8] and higher binding constants are commonly achieved by preorganization of recognition elements at the binding site. Here, we use a common scaffold to impart the same degree of preorganization to all receptors under comparison.

Unlike biological receptors, which function almost exclusively in water, synthetic receptors operate in many solvents, allowing us to modify or enhance intermolecular interactions, such as hydrogen bonding or charge-pairing.[7,9,10] Such interactions can be enhanced by replacing solvents such as water and methanol with aprotic solvents with lower dielectric constants, such as DMSO or chloroform. Even subtle differences—an increase in methanol concentration in an aqueous solution, for instance—can greatly enhance charge-pairing interactions. Therefore, affinity constants can be readily tuned so that a receptor or sensor will work in a desired concentration range. The solvent systems used in this study vary between pure water and 75% methanol to enhance binding.

[a] Dr. S. L. Wiskur, Prof. J. J. Lavigne, Dr. A. Metzger, Dr. S. L. Tobey, Dr. V. Lynch, Prof. E. V. Anslyn
Department of Chemistry and Biochemistry
1 University Station A5300
The University of Texas at Austin
Austin, TX 78712 (USA)

  DOI: 10.1002/chem.200305737

In the design of a synthetic receptor, recognition elements complementary to functional groups on the targeted guest must be incorporated. Our guests of interest contain groups such as carboxylates and/or diols. From precedent, guanidinium ions and boronic acids, respectively, provide excellent complementarity to these functional groups. Ammonium and guanidinium[11] ions associate strongly with carboxylates through hydrogen-bonding and charge-pairing interactions. Ammonium groups have high charge localization,[12] but their geometries are not as conducive as those of guanidinium groups for hydrogen bonding to carboxylates (Figure 1 A). The charge-pairing interactions of guanidinium groups are more diffuse, but they have a more favorable geometry for binding of carboxylates, and remain protonated over a wider pH range (Figure 1 B).[13]

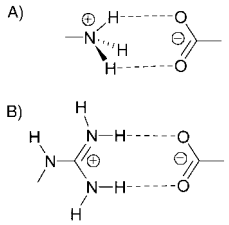

Figure 1. Ammonium groups have geometries less well suited than those of guanidinium groups for hydrogen bonding to carboxylates.

Schmidtchen and co-workers have extensively investigated the thermodynamics of anion recognition by guanidinium groups.[14] They have examined the roles of solvent, counter-anions, and the functionality around the binding site.[15] The association of bicyclic guanidinium structure **1** with benzoate was studied by isothermal titration calorimetry (ITC) to determine counter-anion effects on binding. The binding constant of **1** to benzoate in acetonitrile was greatly affected by the guanidinium's counter-ion. Larger binding constants resulted with the larger, less strongly hydrogen-bonding counter-anions such as hexafluorophosphate. Both enthalpy and entropy were determined to be favorable. Smaller anions resulted in an increase in positive entropy, showing amplification in the release of solvent molecules from the binding site. The exothermic component also decreased with a decrease in the counter-anion size, indicating that the anion was competing with the guest for the guanidinium group.

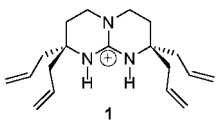

1

Hamilton[16] has also investigated the thermodynamics of guanidinium/carboxylate interactions. In one study, the binding of tetrabutylammonium acetate to a series of guanidinium derivatives was investigated by ITC.[9] The association of the bicyclic guanidinium **2** with acetate had a reasonable affinity in DMSO, but the substitution of the hydrogens for methyl groups in **3** and **4** completely inhibited binding, as found by ITC and ^{1}H NMR, showing the importance of hydrogen bonding for the association. The thermodynamic data showed that the guanidinium/carboxylate interaction was exothermic and displayed positive entropy. The binding was therefore attributed predominantly to hydrogen-bonding interactions, and the affinities were again reduced when the counter-ion was changed from iodide or tetraphenylborate to chloride.

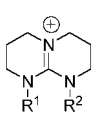

2: R^1=H, R^2=H
3: R^1=CH_3, R^2=H
4: R^1=CH_3, R^2=CH_3

There have been a variety of studies, primarily concerned with sugar recognition, aimed at binding of diols.[17] Some artificial receptors have been designed to form neutral hydrogen bonds to the hydroxy groups of the sugar through amide or alcohol groups, but these receptors generally only work in non-polar, non-hydrogen-bonding solvents.[2,18] Since the binding of saccharides in water is an important endeavor, various groups have developed receptors based on oligosaccharides,[19] oligomers of cyclopentane,[20] and a porphyrin-cryptand system[21] to bind sugars in aqueous media.

The use of boronic acids has advanced the molecular recognition of sugars in aqueous media, because boronic acids form reversible covalent linkages to 1,2- and 1,3-diols (Figure 2 A). Thanks to their ability to form boronate esters,[22] they have been extensively studied for the binding of saccharides and are routinely incorporated into synthetic receptors.[23] The formation of the boronate ester is faster when the boron is tetrahedral, which occurs at high pH. As it is not always desirable to work at high pH, Wulff[24] demonstrated that a tertiary amine adjacent to the boron can add to the boron center, creating a tetrahedral boron at neutral pH (Figure 2 B).

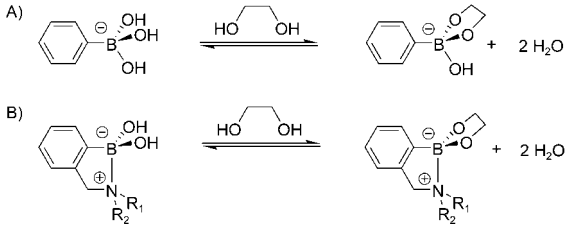

Figure 2. Formation of reversible covalent linkages to diols by boronic acids.

Shinkai and co-workers have performed extensive research into the binding and selectivity of boronic acids with sugars. The fluorescent sensor **5**,[25] which has only one boronic acid moiety, was determined to be selective for fructose. When a second boronic acid is incorporated into the host, however, the host (**6**) now exhibits a preference for glucose.[26] This outcome shows that the spatial orientation of the binding moieties has a significant effect on determining the selectivity of the receptor. Norrild, though, has

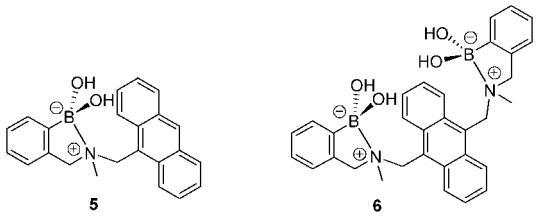

5 **6**

shown that the sugars isomerize when complexed to the boronic acids.[23]

Wang and co-workers have also studied the interactions of boronic acids and diols in detail,[27] by using phenylboronic acid and Alizarin Red S as a fluorescent reporter. They studied buffer effects, pH, and overall affinities of phenylboronic acid for different diols, showing that many common beliefs may actually be misperceptions. For example, it has been stated in the literature that binding constants of these systems are buffer-independent.[28] In their work, Wang et al. showed that the binding constant is dependent on the type of buffer, and in the case of phosphate, the concentration as well. It was also shown that phenylboronic acid has a stronger affinity for catechol than for other 1,2-alkanediols, and that all of their binding constants were pH-dependent.

Although the thermodynamic studies of guanidinium/carboxylate and boronic acid/diol interactions briefly summarized above have been reported, no studies of the result of combining these interactions together have appeared. In the past, our group has designed and studied a series of hosts for sensing of natural products containing both carboxylate and diol moieties. Many of these guests are prevalent in common beverages that humans consume daily, and their concentrations affect characteristics including color, consistency, and perhaps most importantly, flavor.[29–31] The hosts developed for our previous sensing purposes (reviewed briefly below) gave us a series of receptors that allowed an extensive thermodynamic analysis of combinations of guanidinium/carboxylate and boronic acid/diol interactions.

All of the receptors described here are based on a scaffold that induces preorganization of the binding sites. The scaffold is a 1,3,5-trisubstituted 2,4,6-triethylbenzene unit, in which the substituents attached to the methylene groups alternate up and down around the ring, allowing the binding sites to be preorganized on one face of the benzene ring.[32] This steric gearing has been shown to enhance binding in earlier work.[33]

Our first receptor (**7**)[33,34] was designed to bind citrate, a tris-anionic molecule at neutral pH, found in citrus-containing drinks. Selectivity for binding of guests containing three carboxylate moieties was obtained by incorporating three guanidinium groups imbedded in imidazoline groups. Signaling of the binding was achieved by use of an indicator displacement assay (Figure 3),[35] similar to many antibody-based biosensors in competitive immunoassays,[36] and 5-carboxyfluorescein (**11**) was used as the indicator. This host was shown to be selective for citrate over comparable analytes such as sugars and other anions.

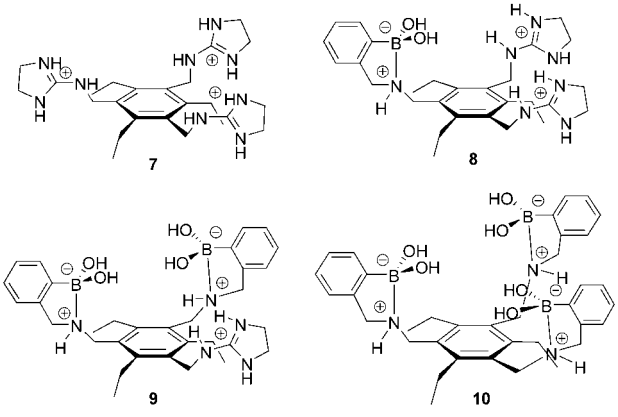

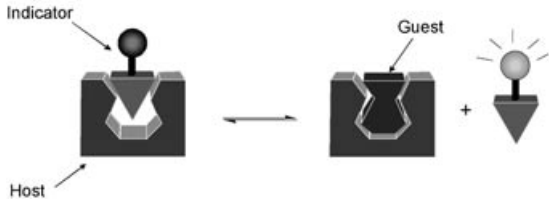

Figure 3. Indicator displacement assay.

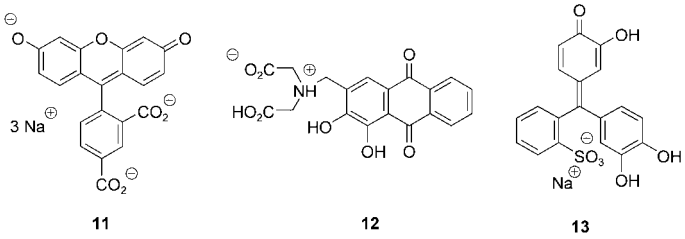

The second receptor **8** was designed to detect tartrate in wines and grape juices.[37] Tartrate contains two carboxylate groups and one diol, so the receptor was designed with two imidazoline-imbedded guanidinium groups and a boronic acid to complex the diol. Alizarin complexone (**12**) was chosen as the indicator for the displacement assay. Host **8** was determined to bind selectively to a combination of tartrate and malate, over other similar analytes, and quantification of a total of these two analytes was achieved in a variety of grape-derived beverages.

Receptor **9** was designed to target gallate, a tris-hydroxybenzoic acid derivative found in Scotch whiskies.[38] The host contained one guanidinium group for binding the carboxylate and two boronic acids for binding the hydroxyphenyl groups. Pyrocatechol violet (**13**) was used as the indicator for binding, and studies showed that **9** was not selective just for gallate, but also bound a class of compounds similar to gallate. All of these analytes are found in Scotch whiskies,[30,31] and are related to the age of the beverage.[31] Through the use of an indicator displacement assay, a correlation was made between the age of the beverage and the response of the sensing ensemble to the class of analytes as a whole.

As alluded to above, in the study reported here, the selectivity of the hosts **7**–**9** was studied in greater detail than in our sensing studies, along with a fourth host (**10**) containing three boronic acid moieties. This study therefore focuses upon a series of receptors with all possible combinations of guanidinium and boronic acid groups, ranging from three guanidinium groups to three boronic acids, all with identical spatial orientations because the scaffold is not altered. The

binding constants of a variety of guests were studied to show the selectivity of each of the hosts. Cooperativity of hosts **8** and **9** with tartrate was also investigated, along with ITC analysis of the hosts to determine the components of the Gibbs free energies of binding. To determine the selectivity of boronic acids for more than just diols, a variety of compounds including amino acids, α-hydroxycarboxylates, and dicarboxylates with a simplified boronic acid compound (**14**) were studied. Lastly, an entropy/enthalpy compensation effect was found for all the hosts and guests. The data provide a unified picture of how hosts **7**–**10** recognize and bind guests containing diol/carboxylate functionalities.

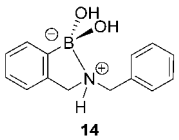

14

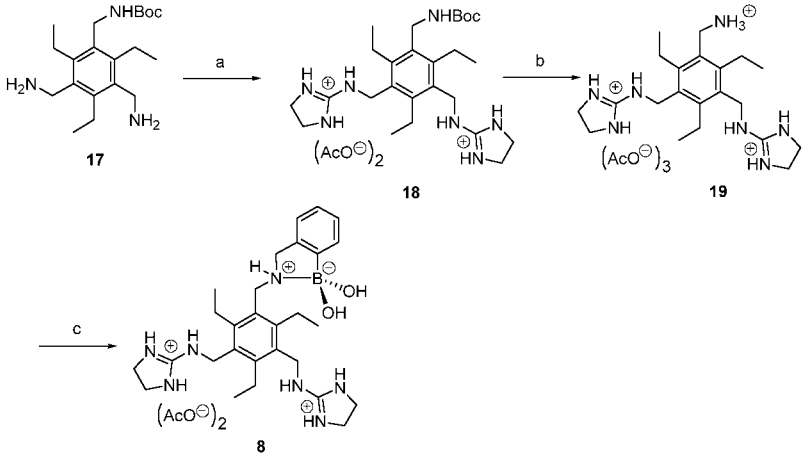

Scheme 3. a) AcOH, 2-methylthio-2-imidazoline, 80 °C, 64 %; b) TFA, H_2O, ion-exchange, 99 %; c) 2-formylbenzeneboronic acid (1.1 equiv), MeOH, 3 Å sieves, $NaBH_4$, 57 %.

Results and Discussion

Synthesis: The synthesis of receptors **7**–**10** began with 1,3,5-tris(aminomethyl)-2,4,6-triethylbenzene (**15**), which was prepared by a three-step synthesis from commercially available 1,3,5-triethylbenzene.[39] The tris-guanidinium host (**7**) was synthesized (Scheme 1) by mixing the triacetate salt of **15** with 2-methylthio-2-imidazoline in a solid melt to obtain **7** as the acetate salt.[32]

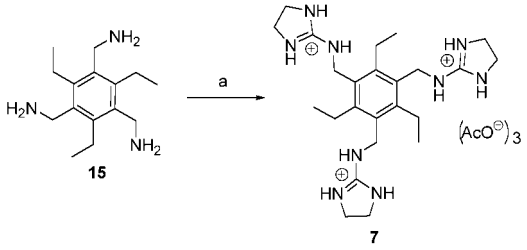

Scheme 1. a) AcOH, 2-methylthio-2-imidazoline, 80 °C, 66 %.

Host **8** was synthesized by protecting one of the nitrogens of **15** with di-*tert*-butyl dicarbonate (Scheme 2) to form a mixture of the di- and monoprotected products (**16** and **17**). From there (Scheme 3), the guanidinium groups were formed by coupling the acetate salt of **17** with 2-methylthio-2-imidazoline by means of another solid melt, resulting in **18**. After deprotection of the Boc-protected amine with trifluoroacetic acid, the amine **19** was alkylated by reductive amination with 2-formylbenzeneboronic acid[37] to complete the synthesis of **8**.

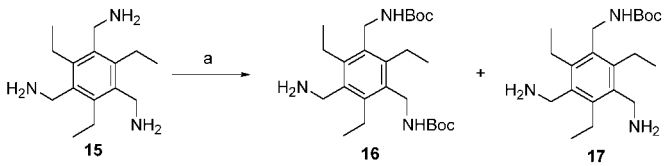

Scheme 2. a) $(Boc)_2O$, $CHCl_3$, **16** (28 %), **17** (18 %).

For the synthesis of the bisboronic acid/monoguanidinium host **9** (Scheme 4), the bis-Boc-protected compound **16** was coupled with an N-Boc-protected imidazoline derivative[40] to form **20**. Subsequent deprotection of the amines and the imidazoline with trifluoroacetic acid (**21**), followed by reductive amination with 2-formylbenzeneboronic acid, afforded **9**.

Compounds **10** and **14** were both created through reductive amination with 2-formylbenzeneboronic acid. The trisboronic acid compound **10** (Scheme 5) was created by using the tris-amine compound **15**, while the single boronic acid compound **14** (Scheme 6) was synthesized from benzylamine.

Binding and structural studies: To determine binding constants, a mechanism to signal the binding, such as the modulation of the spectroscopic properties of a chromophore or fluorophore, needed to be included. In order to signal the presence of a guest, the "signaling site" must communicate with the "binding site". Our group traditionally uses indicator displacement assays to impart the required communication (Figure 3).[34,41] For example, an indicator with binding groups complementary to the receptor of choice is chosen.[34,41] Upon addition of the receptor to the indicator, the spectroscopic properties of the indicator change as it becomes bound to the receptor. This change is due to alteration of the local microenvironment around the indicator. Upon addition of a guest that binds the receptor, the indicator is displaced from the binding site, allowing it to revert to its original spectroscopic properties, and K_a values can be determined from these data.[42]

When looking for an indicator for a particular host, two factors need to be considered. Firstly, in order for the indicator to bind in the cavity, the indicator should have functional groups complementary to the receptor. Secondly, the

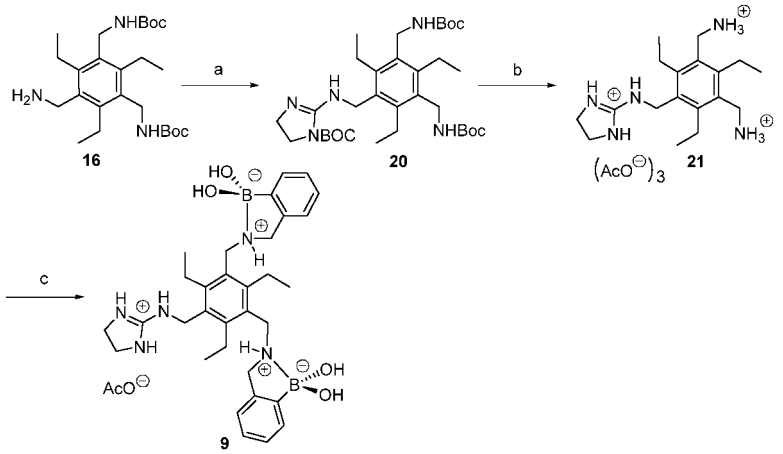

Scheme 4. a) *N*-(1,1-Dimethylethoxycarbonyl)-2-methylthio-2-imidazoline, 5% AcOH in EtOH (*v*/*v*), 60°C, 61%; b) TFA, H_2O, ion-exchange, 98%; c) 2-formylbenzeneboronic acid, MeOH, 3 Å sieves, $HC(OCH_3)_3$, $NaBH_4$, 82%.

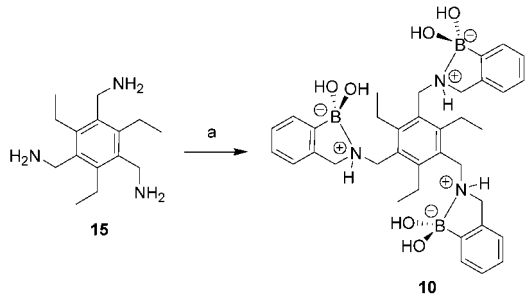

Scheme 5. a) 2-Formylbenzeneboronic acid, MeOH, 3 Å sieves, $HC(OCH_3)_3$, $NaBH_4$, 28%.

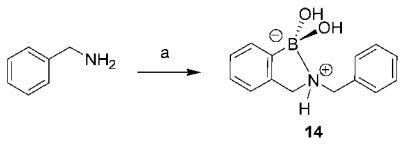

Scheme 6. a) 2-Formylbenzeneboronic acid, $HC(OCH_3)_3$, 3 Å sieves, MeOH, $NaBH_4$, 79%.

indicator should have a pK_a near the working pH, to insure that the indicator is sensitive to microenvironment changes.

All the host/indicator binding constants were determined in the same manner, so only one example of how the association constants are determined is described here. Pyrocatechol violet (**13**) was chosen for the indicator displacement assay with host **9**, due to the catechol and sulfonate moieties, which bind to the boronic acids and the guanidinium, respectively. This indicator is colorimetric and commonly used for the determination of tin and bismuth, in which its color is dependent on its protonation state.[43] Upon addition of **9** to a solution of **13** at constant concentration and pH (Figure 4A), the λ_{max} of the absorbance shifts from 442 to 488 nm. The result was similar to that expected from an increase in pH, which is what was anticipated, since the positive microenvironment of the binding pocket was expected to lower the pK_a of the phenol of the indicator. The data was fit by use of a 1:1 binding algorithm,[42] in which the interaction of **9** and **13** was defined through Equation 1, where I is the concentration of the indicator and L the host.

$$I + L \rightleftharpoons IL \tag{1}$$

Absorbance is defined by Beer's law, and through a derivation of equations using the indicator and ligand mass balance equations and the equilibrium constant, Equation 2 is obtained. The free ligand concentration (L_i) can then be calculated through this quadratic equation, where I_t is the total indicator concentration, K_1 represents the binding constant, and L_t refers to the total ligand concentration. The free ligand concentration is then used in the final binding isotherm (Eq. 3). The calculated delta absorbance and the actual delta absorbance are plotted against the concentration of host. The binding constant (K_1) and the change in molar absorptivity (ε) were iterated until the best fit of the data was obtained (Figure 4B). This gave a binding constant of $6.2\times10^4\,\text{M}^{-1}$ for **9** and **13** in 75% methanol in water (*v*/*v*) at pH 7.4.

$$K_1[L_i]^2 + (1 - K_1[L_t] + K_1[I_t])\,[L_i] - [L_t] = 0 \tag{2}$$

$$\frac{\Delta A}{b} = \frac{\Delta\varepsilon K_1[L_i][I_t]}{[I_t] + K_1[L_i]} \tag{3}$$

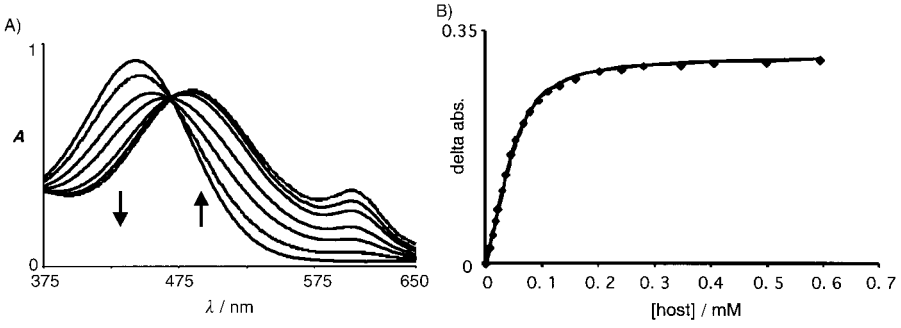

Figure 4. A) UV/Vis spectrum of **13** upon addition of **9**. B) Curve-fitting analysis of the binding of **9** and **13** by use of a 1:1 binding algorithm. The data were taken at 510 nm (75% methanol in water (*v*/*v*), 10 mM HEPES, pH 7.4).

Indicators for the remainder of the hosts were chosen, and all were investigated under the same solvent conditions. To compliment the guanidinium groups of **7**, the pH-sensitive indicator 5-carboxyfluorescein (**11**) was chosen, since the carboxylates should hydrogen bond and form charge pairs to the guanidinium groups, affecting both absorbance and fluorescence upon binding. The binding constant between **7** and **11** was determined to be $4.7\times10^3\,\text{M}^{-1}$. Alizarin complexone (**12**) turned out to be the best indicator for both **8** and **10**, since the boronic acids can form complexes with the dihydroxyphenyl groups, and the guanidinium groups of **8** should interact with the carboxylates on the indicator. The binding constants were calculated to be $2.7\times10^4\,\text{M}^{-1}$ and $4.6\times10^4\,\text{M}^{-1}$ for complexes **8–12** and **10—12**, respectively.

To determine the binding constants of the guests to the receptors we used a competition assay. All the assays work in a similar manner, so again only one specific example is discussed here. Upon addition of gallate to a solution of **9** and **13** at constant concentration and pH (Figure 5A), the absorbance spectra shifted back towards 442 nm as the indicator was displaced from the cavity. The determination of the binding constant is more complicated, due to the equilibria that now exist between the guest (S) and the indicator host complex (IL) (Eq. 4), along with the equilibria from Equation (1).[42]

$$IL + S \rightleftharpoons SL + I \tag{4}$$

For a graphical approach to determine a binding constant between gallate and **9** (K_{11}), the mass balance equations and the equilibrium constants were used to derive the equations that define P (Eq. 5) and Q (Eq. 6).[42] Q is termed the indicator ratio, and can be obtained through the absorbances of the free (A_I) and bound indicator (A_{IL}). These two equations are then used to derive Equation 7, which defines the equation of a line where y is $[S_t]/P$, x is Q, b is 1, and the slope is the ratio of the binding constant of **9–13** (K_1) and **9**-gallate (K_{11}). The data were subsequently fit by varying the value of A_{IL} until the Y intercept was 1, and K_{11} was determined to be $1.0\times10^4\,\text{M}^{-1}$ (Figure 5B).

$$P = \frac{K_{11}[S_t]}{K_1 Q + K_{11}} \tag{5}$$

$$Q = \frac{A - A_{IL}}{A_1 - A} \tag{6}$$

$$\frac{[S_t]}{P} = \frac{K_1}{K_{11}} Q + 1 \tag{7}$$

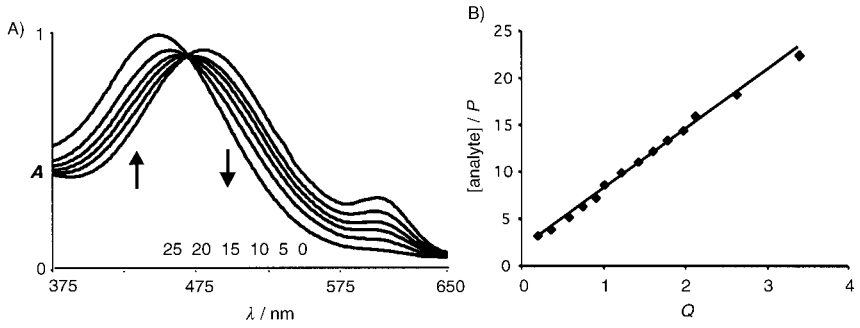

Figure 5. A) UV/Vis spectrum of the complex **9–13** upon addition of gallate. B) Determination of the binding constant of **9** to gallate by a competitive binding algorithm [Eq. (7)]. The data were taken at 605 nm (75% methanol in water (v/v), 10 mM HEPES buffer, pH 7.4).

Each of the hosts **7–10** was tested with a variety of guests (Figure 6) by the indicator displacement method, and the binding constants are listed in Table 1. For receptor **7**, it was

Table 1. Binding constants [M^{-1}] determined for receptors **7–10** by the competition assay (75% methanol in water, 5–10 mM HEPES, pH 7.4).

	7	**8**	**9**	**10**
citrate	6.2×10^4	2.0×10^5	1.8×10^5	2.7×10^4
tartrate	1.7×10^4	5.5×10^4	1.4×10^5	4.0×10^4
malate	1.3×10^4	4.8×10^4	1.5×10^4	8.5×10^3
succinate	3.6×10^3	3.5×10^2	$<1.4\times10^2$	no binding
gallate	<100	2.0×10^4	1.0×10^4	1.0×10^4
3,4-dihydroxybenzoate	<100	1.0×10^4	4.5×10^3	9.0×10^3
lactate	not 1:1	5.0×10^2	5.0×10^2	1.1×10^3
glucose	no binding	1.6×10^2	1.4×10^2	9.0×10^2
fructose	no binding	3.0×10^2	4.0×10^2	6.0×10^2
catechin	no binding	8.0×10^2	5.7×10^2	5.0×10^2
EGCg	no binding	4.5×10^3	5.2×10^3	6.0×10^3

expected that the guests that were highly anionic would give the strongest interactions and that the guests that were neutral would not bind with the guanidinium groups. It was found that citrate, which has three carboxylates, was the guest with the highest binding constant; one possible binding motif (**A**), observed in the obtained crystal structure,[32] with all three carboxylates of citrate hydrogen-bonded to the guanidinium groups of **7** is shown. Guests with two carboxylates, such as tartrate, malate, and succinate, were also strong binders with **7**. Malate and tartrate, which also have one and two hydroxy groups, respectively, had binding constants three to four times weaker than their three-carboxylate counterpart. Succinate, which has no hydroxy groups, had a binding constant with **7** over an order of magnitude weaker than that of citrate. The binding affinities of **7** with monocarboxylate-containing guests such as 3,4-dihydroxybenzoate and gallate were so low that they were estimated to be less than $100\,\text{M}^{-1}$. The other monocarboxylate guest, lactate, was determined to bind **7** with a higher stoichiometry, with more than one guest bound in the cavity. Other guests containing only hydroxy or catechol functionalities—such as fructose, glucose, catechin, and epigallocatechin gallate

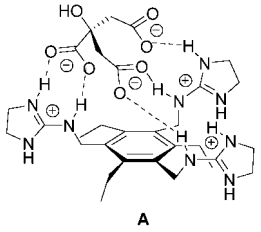

A

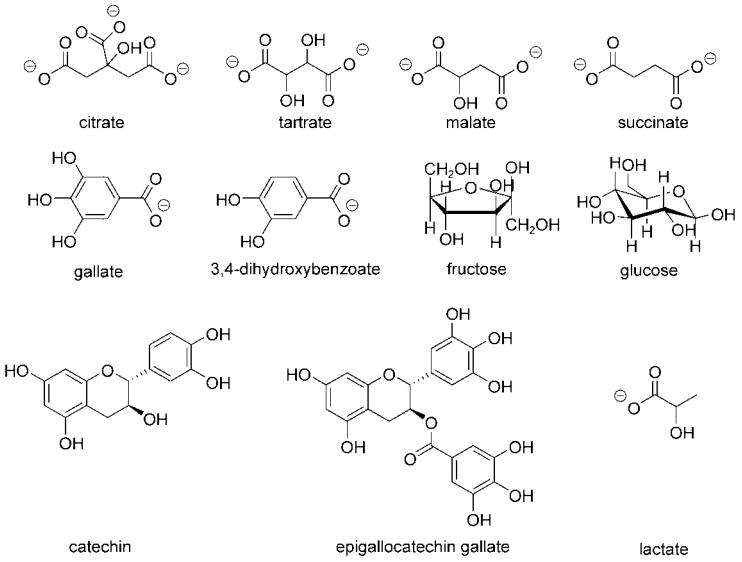

Figure 6. Guests tested for affinities with receptors **7**–**10**.

(EGCg)—were not expected to bind to **7** and indeed had no detectable binding interactions.

It was expected that guests possessing two carboxylates and one diol should show optimum binding with receptor **8**. Tartrate was the guest of choice, and indeed bound strongly to the receptor. Malate, similar in structure to tartrate but with one hydroxy group fewer, however, had an almost identical affinity to the receptor. Citrate bound **8** with an affinity almost four times stronger than that of tartrate, indicating that the carboxylates of citrate were interacting with the boronic acid. Succinate, a malate equivalent but without any hydroxy group, had a significantly decreased affinity for **8**, by almost two orders of magnitude. This indicated that the α-hydroxycarboxylate functionality has a greater affinity for boronic acids[44,45] than 1,2-alkanediols. The binding of α-hydroxycarboxylates by boronic acids has been demonstrated in work by Houston and co-workers with Shinkai's boronic acid receptor.[45] The receptor had a high affinity for tartrate, the affinity for malate was lower, and no binding was detected with succinate. The possible binding conformation of **8** to an α-hydroxycarboxylate versus a diol is depicted in Scheme 7. Here the binding of the α-hydroxycarboxylate of tartrate to the boronic acid of **8** (**B**) is depicted in equilibrium with the formation of the boronate ester between the boronic acid and the diol (**C**). The fact that tartrate and malate have very similar binding constants with **8** gives evidence for **B** being the more favorable binding motif for tartrate. However, it is likely that both binding modes exist in solution. Structure **D** is proposed for malate bound to **8** in solution.

The binding constants of gallate and 3,4-dihydroxybenzoate with receptor **8** were also of the same order of magnitude as those of tartrate and malate. This similarity is due to the catechol/boronic acid interactions, which are known to be stronger than those of vicinal diols.[22,27] The larger neutral catechol-containing guests (catechin and EGCg) had binding affinities with **8** an order of magnitude weaker than those of the aromatic carboxylates. Simple sugars, such as fructose and glucose, bound with even lower binding constants, since the interaction with the receptor is solely with the single boronic acid.

The same guests were tested with receptor **9**, which has two boronic acid moieties and one guanidinium. Citrate and tartrate had the strongest affinities for the receptor, while malate's affinity was an order of magnitude less. Again, this difference indicates that the boronic acids are preferentially interacting with the α-hydroxycarboxylates. Scheme 8 depicts the possible binding interactions of tartrate and malate with **9**. With tartrate, two α-hydroxycarboxylate interactions with the two boronic acids can be represented (**E**), along with a structure in equilibrium possessing a boronate ester

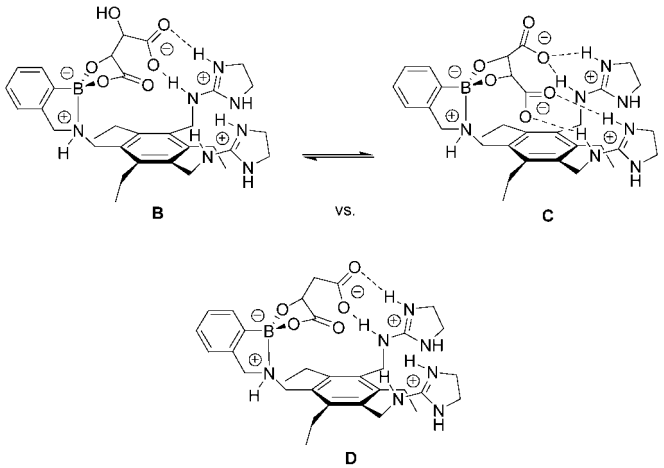

Scheme 7. Binding of the α-hydroxycarboxylate of tartrate to the boronic acid of **8**.

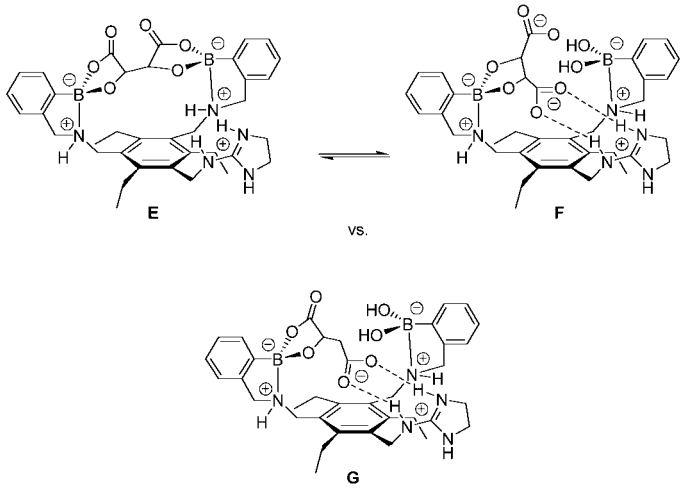

Scheme 8. Possible binding interactions of tartrate and malate with **9**.

(**F**). In **F**, the interaction between the carboxylate and the boronic acid could be either hydrogen bonding, or coordination of the carboxylate to the boron, making a mixed anhydride (not shown). With malate (**G**), only one α-hydroxycarboxylate interaction with a boronic acid can exist, which results in the lower binding affinity with **9**.

Gallate bound **9** with an affinity of the same order of magnitude as malate, again showing the greater affinity of 1,2-dihydroxyphenyl groups over 1,2-alkanediols. EGCg was an order of magnitude higher than catechin in its binding constant with **9**, presumably due to the increased number of hydroxy groups. EGCg's similar binding affinity to 3,4-dihydroxybenzoate again shows the importance of the catechol functionalities, whereas the affinities of glucose and fructose were an order of magnitude less.

The tris-boronic receptor **10** again showed selectivity for the guests with α-hydroxycarboxylate systems, such as tartrate. Citrate, which only has one α-hydroxycarboxylate, had a binding constant with **10** comparable to that of tartrate, which was attributed to interaction with the boronic acids by the other two carboxylates of citrate. The affinity of **10** for malate was five times weaker than for tartrate, due to the one fewer hydroxy group. The possible binding modes of tartrate are illustrated in Scheme 9, showing the formation of a boronate ester (**I**) versus the binding of the α-hydroxycarboxylates (**H**). In structure **I**, the actual interaction between a carboxylate and boronic acid is not known, but a mixed anhydride between the carboxylate and the boron is a possibility. A binding mode for malate similar to those shown in Scheme 7 and Scheme 8 can be assumed, highlighting the increased number of favorable binding interactions for tartrate. Importantly, without the alcohol moieties (succinate) no binding to this receptor could be detected, suggesting that the dicarboxylates are not interacting with the boronic acids.

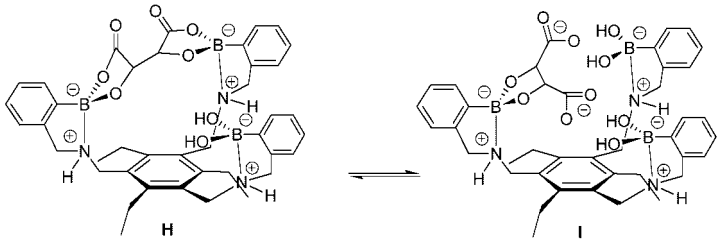

Scheme 9. Possible binding modes of tartrate with **10**.

Both gallate and 3,4-dihydroxybenzoate had affinity constants with **10** of the same order of magnitude as malate, showing the strong interactions of the boronic acids with the catechols. The simple alkanediols (glucose and fructose) had the lowest affinities with **10**.

From analysis of all the binding constants discussed above, it became clear that the boronic acids were playing more of a role than just binding vicinal diols.[44,45] We therefore turned our attention more closely to the role of the boronic acids. After analysis of the guests tested with hosts **8**–**10**, a series of simpler guests with a simplified boronic acid compound **14** were analyzed. Since **14** does not possess a signaling site, the competition assay was also employed, with **12** as the indicator. The determined binding constants are shown in Table 2, along with the binding constant of **12** with **14**. Aliphatic diols have been widely examined with boronic acids; however, catechols have not been as widely tested,[22,27] so this was our starting point. Since **12** bound strongly, the iminodiacetate[46] functionality was tested to determine whether the boronic acid was binding through the catechol or the side arm of **12**. However, the binding of this guest with **14** was too weak to be determined. Diethanolamine, the alcohol equivalent to iminodiacetate, was also tested, but also had weak binding. Because citrate bound hosts **8**–**10** better than expected, the interaction of lactate, an α-hydroxycarboxylate, was tested, and it was shown to have an excellent binding affinity for the boronic acid in **14**. The amino acid[47] equivalent alanine had very little affinity with the receptor, showing that the alcohol is preferred over an amine. Malonate also showed a strong affinity for **14**, indicating that binding through the two carboxylates was also possible,[48] forming a six-membered ring. When any simple aliphatic diols such as ethylene glycol or *cis*-1,2-cyclohexanediol were attempted, binding was always too low to determine. It was therefore determined that a simple boronic acid (**14**) has high affinities for α-hydroxycarboxylates, catechols, and dicarboxylates that can form six-membered rings, over amino acids and simple 1,2-alkanediols.

Table 2. Binding constants [M^{-1}] determined for **14** by competition assay with the indicator alizarin complexone (75% methanol in water, 10 mM HEPES, pH 7.4).

	14
alizarin complexone (**12**)	4.4×10^3
malonate	8.6×10^2
lactate	3.1×10^2
alanine	<50
iminodiacetic acid	<50
catechol	4.0×10^2
cis-1,2-cyclohexanediol	<50
diethanolamine	75

To investigate the geometry at the boron center, a crystal structure of **14** was obtained (Figure 7). As can be seen, the nitrogen has added onto the boron, making the boron tetrahedral. The protonated state of the nitrogen exists, as the hydrogen on the nitrogen is still present,[49] allowing the secondary nitrogen and the boron to form a zwitterionic complex. The use of boronic acids with adjacent amines in sensors is routinely performed with tertiary amines.[25,50] This helps to show the potential of incorporation of a secondary amine for sensor applications.[51]

Enthalpy and entropy: Given that the selectivity of the hosts had been determined, along with some structural insight, we were interested in the driving force for the binding of hosts **7**–**10** and **14**. The Gibbs free energies of binding can be calculated from the K_a values, but in order to divide ΔG^0 into its parts, enthalpy and entropy, isothermal titration calorimetry (ITC) was used. This method measures the heat

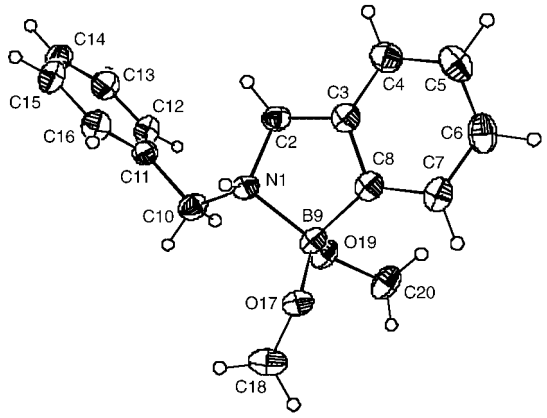

Figure 7. View of **14**, showing the atom labeling scheme. Displacement ellipsoids are scaled at the 50% probability level.

were obtained in 75% methanol in water. Ion-pairing interactions are reduced in pure water, and in addition the increased buffer concentration lowers binding affinities.

The data show that binding is driven by a combination of entropy and enthalpy, both being favorable. In many systems, exothermic enthalpy is associated with charge-pairing interactions or tight binding interactions that result in structural tightening, while positive entropy is generally associated with a release of solvent into bulk solution. Negative entropy can result from the cost of freezing intermolecular motion. With regard to the binding of **7** and citrate in pure water with a phosphate buffer, the majority of the driving force is derived from entropic contributions, indicating a large release of solvent upon **7** binding citrate.[32,53]

The binding between **8** and tartrate was determined to be exothermic with positive entropy. The increase in the enthalpic component versus **7**'s binding of citrate indicates stronger interactions between **8** and tartrate. The covalent bonds between the boronic acid and tartrate (Scheme 7, **B** and **C**) might contribute to the enthalpic component relative to the hydrogen-bonding and charge-pairing interactions of **7**. Further, the entropic component is still present with **8**, which could result from the release of solvent from the binding pocket and the guest. The binding of the carboxylates of tartrate to the guanidinium groups of **8** displace water into bulk solvent. Additionally, two water molecules are also released for each boronate ester formed from either the diol or the α-hydroxycarboxylates.

A large enthalpic component with a small entropic component was determined for the binding of **9** to tartrate. The possibility of formation of four reversible covalent bonds to tartrate exists (Scheme 8, **E**), making the complexation exothermic, but resulting in a more ordered host/guest complex, lowering the entropy of binding relative to **7** and **8**. The rigidity of the host/guest complex induces a loss of entropy, which must outweigh the increased entropy from the displacement of solvent from the binding cavity, lowering the overall entropy of binding.

The binding of **10** with tartrate had a driving force similar to that of receptor **8**'s binding of tartrate, where the enthalpy and entropy were both favorable. The formation of complex **H** (Scheme 9) has **10** binding tartrate in an orientation similar to **9** (Scheme 8, **E**), yet the exothermicity with **10** has decreased and there is more favorable entropy. Perhaps the rigidity in the binding of tartrate to **10** is not as pronounced as for tartrate to **9**, due to subtle size and shape differences in the binding cavities. Without the increase in rigidity, not as much entropy is lost and the displacement of solvent into bulk solution has a more pronounced effect.

Table 3. ITC analysis of **7** (100% water, pH 7.4, 103 mM phosphate buffer),[53] **8**–**10** (100% water, pH 7.4, 50 mM HEPES), and **14** (100% water, pH 7.4, 250 mM HEPES).

	7·citrate	**8**·tartrate	**9**·tartrate	**10**·tartrate	**14**·catechol	**14**·malonate
ΔH^0 [kcal mol^{-1}]	−0.2	−1.6	−2.9	−1.5	−1.4	0.02
$T\Delta S^0$ [kcal mol^{-1}]	3.3	2.1	0.6	1.8	1.8	4.2
ΔG^0 [kcal mol^{-1}]	−3.6	−3.7	−3.5	−3.3	−3.2	−4.2
K_a [M^{-1}]	4.4×10^2	5.2×10^2	3.7×10^2	2.6×10^2	2.2×10^2	1.2×10^3

evolved or absorbed upon binding, deriving K_a, ΔG^0, ΔH^0, and ΔS^0 in a single experiment.[52] The instrument measures the change in heat of a system upon addition of an aliquot of guest into a solution of host. This heat exchange is shown in Figure 8 (top) for the addition of tartrate into a solution of **8** at pH 7.4 (100% water, 50 mM HEPES buffer, 25 °C). Integration of the exothermic peaks leads to the binding curve shown at the bottom of Figure 8. Use of a one-site binding model to fit the data leads to the values shown in Table 3. The association constant between tartrate and **8** was found to be significantly lower than that reported in Table 1. This can be attributed to the performing of the ITC experiments in 100% water, while the UV/Vis studies

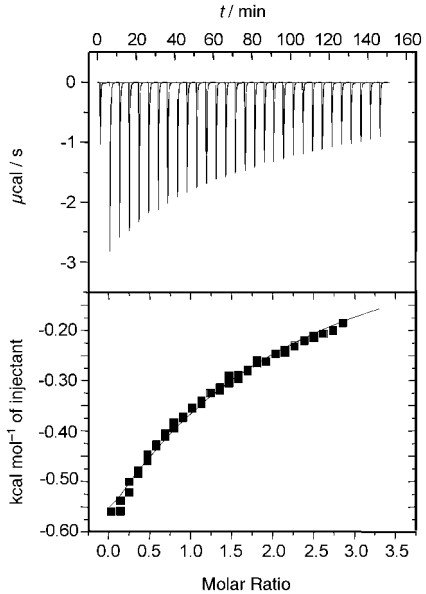

Figure 8. ITC analysis of **8** with tartrate (100% water, 50 mM HEPES buffer, pH 7.4).

With the boronic acid model compound **14**, the association of catechol, malonate, and lactate were analyzed by ITC. Catechol was both entropy- and enthalpy-driven, with exothermic binding and positive entropy. Malonate, on the other hand, was primarily entropy-driven (positive), with enthalpy being slightly endothermic. If these two studies are viewed in terms of rigidity, it would appear that the formation of the boronate ester with catechol results in a more rigid complex than malonate binding **14**. This rigidity reduces the entropy of the system, even though two solvent molecules are being released for each boronate ester formed. Lactate is not reported, due to the fact that no accurate association constant could be obtained, because of small changes in the heat, which means that the binding is almost entirely entropy-driven.

If the entropy and enthalpy of binding for each of the receptors are plotted together (Figure 9), the result is a straight line. This phenomenon is termed enthalpy/entropy

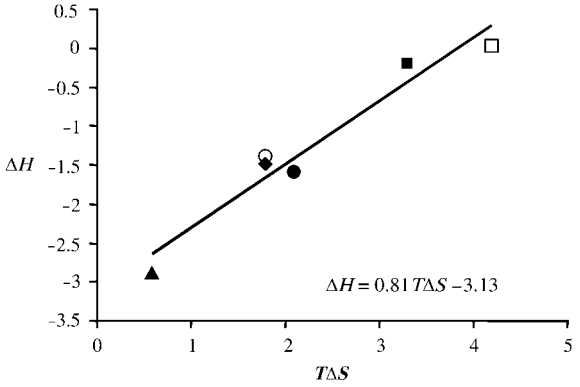

Figure 9. Enthalpy (ΔH^0, kcal mol^{-1}) vs entropy ($T\Delta S^0$, kcal mol^{-1}) compensation plot for hosts **7–10** and **14**, binding different guests; □: **14**•malonate, ○: **14**•catechol, ■: **7**•citrate, ●: **8**•tartrate, ▲: **9**•tartrate, ◆: **10**•tartrate.

compensation (EEC), an effect that reflects how increasing favorable enthalpy is offset by a change in entropy or vice versa, resulting in a small change in free energy. For example, as the rigidities of the host/guest complexes increase, the disorder in the complexes decreases, resulting in a compensation of the increase in enthalpy. This effect can be seen in receptors **7–9**, as the binding sites of the receptors change from three guanidinium groups to two boronic acids and one guanidinium group. The slope of the EEC graph was determined to be 0.8, which means that the free energy of binding is more sensitive to changes in entropy.[54] A slope of less than one suggests that in the rational design of a receptor to bind with better binding contacts to the host, the increased exothermicity of binding (ΔH^0) would be defeated by the compensating entropy ($T\Delta S^0$).

It is interesting that receptors containing both boronic acids and guanidinium groups lie on the same plot, with the same slope. This means that the extents to which the increased enthalpies of binding are offset by lower entropy must be nearly identical for the two molecular recognition motifs. Ion-pairing of a carboxylate with a guanidinium and reversible binding of α-hydroxycarboxylates with boronic acids act similarly in this regard, at least in the series of receptors studied. More work is required to see if this is a general phenomenon.

Cooperativity: Studies to explore cooperativity of receptors **8** and **9** in binding of various guests were performed. Cooperativity, in the case of receptor **8**, is defined as enhanced or diminished binding interactions of the boronic acid and the two guanidinium groups to the diol and carboxylates of tartrate, respectively. The method proposed by Jencks[55] was used to analyze the two receptors. The guest to be studied is divided into parts A and B, where the receptor can independently bind both of these, such that the parts can be compared to the whole to determine whether the binding is cooperative when they are connected. Here, the Gibbs free energy of connection (ΔG_s^0) is defined as the change that results from the connection of A and B, and can be determined from the difference between the Gibbs free energy of the parts minus the Gibbs free energy of the whole [Eq. (8)] or the binding constants [Eq. (9)]. Positive cooperativity would be shown by a positive ΔG_s^0, which is a gain in free energy from binding of AB vs. binding of A and B separately. The opposite is true for a negative ΔG_s^0.

$$\Delta G_s^0 = \Delta G_A^0 + \Delta G_B^0 - \Delta G_{AB}^0 \quad (8)$$

$$\Delta G_s^0 = RT \ln \frac{K_{AB}}{K_A K_B} \quad (9)$$

For receptors **8** and **9**, the binding of tartrate was studied. Two lactates were chosen to study the α-hydroxycarboxylate interactions with the boronic acids and the guanidinium groups. Lactate's binding constant with **8** was determined to be 500 M^{-1}, which gave a ΔG_s^0 of −0.9 kcal mol^{-1} for tartrate, which is indicative of negative cooperativity.

The cooperativity of binding with regard to receptor **9** and tartrate was also analyzed. The association constant between **9** and lactate was determined to be 500 M^{-1}, which gave a ΔG_s^0 of −0.3 kcal mol^{-1} for tartrate, negative but close to zero cooperativity.

One must remember that both negative and positive cooperativity give enhancements in the binding affinities. Negative cooperativity merely suggests that the enhancement was not as large as could have been achieved. The fact that there is only a small negative cooperativity in free energy with the lactate as the parts suggests equal free energy interactions from each of the α-hydroxycarboxylates of tartrate when binding to **9**.

Conclusion

Guanidinium groups and boronic acids have previously been investigated for binding carboxylates and diols, respectively. We have analyzed four receptors **7–10** that incorporate these functionalities individually and together, examining the thermodynamics of binding, selectivities, and cooperativity. The trisguanidinium receptor **7** gave a predictable selectivity for highly anionic analytes. Receptors **8–10**, which in-

corporated boronic acids, had higher affinities for guests that possessed α-hydroxycarboxylate and catechol functionalities over simple alkane-1,2-diols. The study of a monoboronic acid compound **14** confirmed the high affinity for α-hydroxycarboxylates and catechols. Isothermal titration calorimetry revealed that the binding of citrate and tartrate with hosts **7**–**10** were all exothermic, with positive entropy. The boronic acids appear to add an enthalpic component to the thermodynamics of binding, along with an entropy component due to the release of water. However, the binding with boronic acids also leads to more tightly bound complexes, while the complexes with guanidinium groups are looser and have larger entropic components related to solvent release. Our data show that an enthalpy/entropy compensation phenomenon exists between the guanidinium and the boronic acid hosts. This indicated that the offset of enthalpy for losses in entropy for guanidinium groups and boronic acids were essentially the same for our hosts. The cooperativity of tartrate binding to **8** and **9** was also investigated. It was determined that **9** had a binding pocket that was complementary for the binding of tartrate, showing only small negative cooperativity.

Experimental Section

General: All reagents were obtained from Aldrich, and were used with no further purification unless otherwise noted. Methanol was distilled from over magnesium, and triethylamine was distilled from one calcium hydride when noted. Products were placed under high vacuum for at least 12 h before spectra were obtained. ^{1}H and ^{13}C NMR spectra were obtained on a Varian Unity Plus 300 MHz spectrometer. ^{11}B NMR spectra were obtained on a Bruker AMX 500 spectrometer. A Finnigan VG analytical ZAB2-E spectrometer was used to obtain high-resolution mass spectra, UV/Vis spectra were collected on a Beckman DU640 spectrophotometer, and isothermal titration calorimetry was performed on a VP-ITC MicroCalorimeter instrument (MicroCal).

UV/Vis titrations of indicator and receptor: All solutions were buffered at pH 7.4 with HEPES buffer (5 mM) in methanol in water (75 % *v*/*v*). A solution of 5-carboxyfluorescein (23 μM) was prepared in the cuvette, and a stock solution of **7** (500 μM) and 5-carboxyfluorescein (23 μM) was titrated into this, with the indicator concentration being kept constant. The data was recorded at 498 nm to determine the association constant. The rest of the host/indicator association constants were determined in a similar manner with differences in concentrations. Alizarin complexone–**8** (10 mM HEPES, 150 μM of indicator, 1.6 mM of **8**, 525 nm); pyrocatechol violet–**9** (10 mM HEPES, 60 μM of indicator, 1.2 mM of **9**, 510 nm); alizarin complexone–**10** (10 mM HEPES, 150 μM of indicator, 1.2 mM of **10**, 525 nm); and alizarin complexone–**14** (10 mM HEPES, 150 μM of indicator, 2.8 mM of **14**, 525 nm).

UV/Vis titrations of receptor/indicator ensemble and guests: All solutions were buffered at pH 7.4 with HEPES buffer (5–10 mM) in methanol in water (75 % *v*/*v*). A solution of indicator (**11**, 14 μM) and receptor (**7**, 74 μM) was prepared in the cuvette, and a stock solution of indicator, host, and guest, was titrated into this, with the indicator and host concentrations being kept constant. The data were taken at the appropriate wavelength to determine the association constant. The guest concentration in the stock solution varies between 5–80 times the concentration of host. Alizarin complexone–**8** (10 mM HEPES, 150 μM of indicator, 170 μM of **8**, 525 nm); pyrocatechol violet–**9** (10 mM HEPES, 60 μM of indicator, 260 μM of **9**, 510 or 605 nm); alizarin complexone–**10** (10 mM HEPES, 150 μM of indicator, 185 μM of **10**, 525 nm); and alizarin complexone–**14** (10 mM HEPES, 150 μM of indicator, 470 μM of **14**, 525 nm).

Isothermal titration calorimetry of receptors 8, 9, and 10 with tartrate: All solutions were buffered at pH 7.4 with HEPES buffer (50 mM) in 100 % water. The calorimetry cell contained the receptor (1.0 mM), and tartrate (21.4 mM) was titrated into the cell. A total of 30 injections were made at a volume of 6 μL per injection and a spacing of 300 seconds between injections. The solution was constantly stirred and kept at 25 °C. The heat of dilution was measured by titration of the tartrate solution, in the same fashion as above, into a solution of just buffer. The heat of dilution data were subtracted from the raw titration data to produce the final binding curve. The data were fit with a one-site binding model with Origin software version 5.0. The other ITC experiments were all performed in a similar manner, with variations in buffers and concentrations.

1-(*N*-(*ortho*-Boronobenzyl))aminomethyl-2,4,6-triethyl-3,5-((2-imidazolin-2-yl-amino)methyl)benzene (8): 1-Aminomethyl-2,4,6-triethyl-3,5-((2-imidazolin-2-yl-amino)methyl)benzene (300 mg, 0.53 mmol, 1 equiv) was mixed with 2-formylbenzeneboronic acid (87.6 mg, 0.58 mmol, 1.1. equiv) in anhydrous methanol. Distilled triethylamine (360 μL, 2.65 mmol, 5 equiv) and 5–10 activated molecular sieves (3 Å) were added, and the solution was stirred at 25 °C for 3 h. After this time, sodium borohydride (20.2 mg, 0.53 mmol) was added, and the solution was stirred for an additional 1 h. The solution was filtered through a pad of celite to remove the sieves, the filter cake was washed with methanol and trimethyl orthoformate, and the solvent was removed by rotary evaporation. The resulting residue was placed under reduced pressure (6 mm Hg) for two days to remove the trimethylborate. This residue was then dissolved in water and filtered through a pad of celite to remove the reduced aldehyde. The water was lyophilized off, resulting in a fluffy white solid (366 mg, 99 %). M.p. 197 °C (decomp); ^{1}H NMR (300 MHz, CD_3OD, 25 °C): δ = 1.12 (t, 6H; CH_3); 1.23 (t, 3H; CH_3), 1.81 (s, 9H; CH_3), 2.74 (q, 2H; CH_2), 2.82 (q, 4H; CH_2), 3.75 (s, 8H; CH_2), 3.97 (s, 4H; CH_2), 3.75 (s, 8H; CH_2), 3.97 (s, 2H; CH_3), 4.11 (s, 2H; CH_2), 4.43 (s, 4H; CH_2), 7.11 (d, 1H; Ph), 7.15–7.23 (m, 2H; Ph), 7.49 (d, 1H; Ph) ppm; ^{13}C NMR (75 MHz, CD_3OD, 25 °C): δ = 16.4, 16.6, 23.1, 24.1, 42.0, 44.1, 53.5, 116.2, 127.9, 128.4, 130.8, 131.4, 146.7, 161.2, 162.8, 178.8 ppm; ^{11}B NMR (160 MHz, CD_3OD, 25 °C): δ = 8.2 ppm; HMRS (FAB(gly)) (note; as the glycerolboronate ester): *m*/*z*: calcd for $C_{31}H_{47}BN_7O_3$: 576.3833; found: 576.3839 $[M+H]^+$.

1,3,5-Tris[(2-benzeneboronic acid)aminomethyl]-2,4,6-triethylbenzene (10): Dry triethylamine (1.0 mL) and 2-formylbenzeneboronic acid (0.33 g, 2.19 mmol) were added to a solution of **15** (0.16 g, 0.63 mmol) in dry methanol over molecular sieves (3 Å) in an inert atmosphere. The reaction mixture was heated to 45 °C for 6 h. Sodium borohydride (0.18 g, 4.76 mmol) was added, and the reaction mixture was allowed to cool to room temperature. The mixture was filtered through celite and the solvent was removed. The solid was dissolved in water, filtered through celite, and lyophilized. Trimethyl orthoformate (2 mL) and dry methanol were then added, the mixture was stirred for 2 h, and the resulting residue was placed under vacuum for an additional 24 h. The final purification step involved dissolving of the solid with a mixture of ethyl acetate/methanol (9:1) and filtration through celite. The solvent was removed to yield a white solid (0.12 g, 28 %). M.p. 230 °C (decomp); ^{1}H NMR (CD_3OD, 300 MHz): δ = 7.49 (d, 3H), 7.1–7.2 (m, 9H), 4.05 (s, 6H), 4.02 (s, 6H), 2.98 (q, 6H), 1.07 (t, 9H) ppm; ^{13}C NMR (CD_3OD, 75 MHz): δ = 157.1, 148.2, 143.2, 132.7, 129.2, 128.7, 125.6, 54.8, 45.3, 25.3, 17.6 ppm; ^{11}B NMR (CD_3OD, 160 MHz, 25 °C): δ = 10.0 ppm; HRMS-CI$^+$: *m*/*z*: calcd for $C_{39}H_{48}B_3N_3O_3$: 639.399; found: 639.397 (dehydrated methoxy form).

1-(*N*-(*ortho*-Boronobenzyl))aminomethylbenzene (14): 2-Formylbenzeneboronic acid (0.158 g, 1.05 mmol) was dissolved in distilled methanol (20 mL) under argon. To this were added benzylamine (126 μL, 1.18 mmol), triethylamine (1 mL, 13.84 mmol), and molecular sieves (3 Å). The solution was stirred slowly at 40 °C for 4 h. Sodium borohydride (0.098 g, 2.6 mmol) was added, and the reaction mixture was stirred for another 12 h. The solution was filtered through celite. The filtrate was stirred with trimethyl orthoformate and a few drops of acetic acid for 5 h, and the solution was evaporated under reduced pressure. The residue was stored under reduced pressure (5–10 mTorr) for two days to remove any remaining trimethoxyborane. The final purification step involved dissolving of the solid with a mixture of ethyl acetate/methanol (9:1) and filtration through celite. The resulting solid was dissolved in water and lyophilized to yield a white fluffy solid (0.2 g, 79 %). M.p. (decomp); ^{1}H NMR ($CDCl_3$, 300 MHz): δ = 1.94 (s, 3H), 3.86 (s, 2H), 3.98 (s, 2H), 7.07 (m, 1H), 7.18 (m, 2H), 7.43 (m, 6H) ppm; ^{13}C NMR ($CDCl_3$,

75 MHz): δ = 22.3, 52.1, 54.1, 127.7, 128.3, 129.5, 129.9, 130.8, 131.6, 136.2 ppm; ^{11}B NMR (CD_3OD, 160 MHz, 25 °C): δ = 10.3 ppm; HR-MS-CI$^+$: *m/z*: calcd for $C_{14}H_{15}BNO$: 224.125; found: 224.124 (dehydrated form).

1,3-Bis[[(1,1-dimethylethoxy)carbonyl]aminomethyl]-5-aminomethyl-2,4,6-triethylbenzene (16): A solution of di-*tert*-butyl dicarbonate (1.74 g, 7.8 mmol) in chloroform was added dropwise to **15** (2.48 g, 10.0 mmol) in chloroform. The mixture was allowed to stir for 12 h. The solvent was removed, and separation was performed by column chromatography (silica gel, gradient of 1–20% ammonia sat. methanol in CH_2Cl_2); yield: 1.25 g, 28%; m.p. 150–154 °C; ^{1}H NMR (300 MHz, CD_3OD): δ = 4.27 (s, 4H), 3.84 (s, 2H), 2.75 (q, 6H), 1.45 (s, 18H), 1.16 (t, 9H) ppm; ^{13}C NMR (75 MHz, $CDCl_3$): δ = 156.17, 143.41, 138.08, 133.03, 80.17, 40.19, 39.57, 29.17, 23.49, 17.42 ppm; HRMS-CI$^+$: calcd for $C_{25}H_{43}N_3O_4$: 450.333; *m/z*: found: 450.332.

1-[[(1,1-Dimethylethoxy)carbonyl]aminomethyl]-3,5-aminomethyl-2,4,6-triethylbenzene (17): A solution of di-*tert*-butyl dicarbonate (1.74 g, 7.8 mmol) in chloroform was added dropwise to **15** (2.48 g, 10.0 mmol) in chloroform. The mixture was allowed to stir for 12 h. The solvent was removed, and separation was performed by column chromatography (silica gel, gradient of 1–20% ammonia sat. methanol in CH_2Cl_2); yield: 0.63 mg, 18%; m.p. 120–125 °C; ^{1}H NMR (300 MHz, $CDCl_3$): δ = 4.61 (brs, 1H; NHBoc), 4.29 (s, 2H), 3.82 (s, 4H), 2.75 (q, 6H), 1.40 (s, 9H), 1.30 (s, 4H), 1.17 (t, 9H) ppm; ^{13}C NMR (75 MHz, $CDCl_3$): δ = 156.17, 141.89, 137.47, 132.38, 79.58, 39.76, 39.08, 28.68, 22.95, 17.05, 16.92 ppm; HRMS-CI$^+$: *m/z*: calcd for $C_{20}H_{36}N_3O_2$ 350.281; found: 350.281.

1-[[(1,1-Dimethylethoxy)carbonyl]aminomethyl]-3,5-(4,5-dihydro-1*H*-imidazol-2-yl)aminomethyl-2,4,6-triethylbenzene (18): The acetate salt of **17** (0.350 g, 0.75 mmol) was ground together with 2-methylthio-2-imidazoline (0.18 g, 1.53 mmol) and packed in a conical vial, sealed, and heated to 100 °C for 3 d. The solid was then dissolved in 5% acetic acid (aq.) and lyophilized. Purification was performed by FPLC (C18 modified silica gel; particle size 55–105 μm) and eluted with an NH_4Ac/CH_3CN gradient from 100% NH_4Ac (25 mM) to neat CH_3CN (0.29 g, 64%). M.p. 250 °C (decomp); ^{1}H NMR (300 MHz, $CDCl_3$): δ = 4.43 (s, 4H), 4.32 (s, 2H), 3.76 (s, 8H), 2.74 (q, 6H), 1.89 (s, 6H), 1.45 (s, 9H), 1.19 (t, 9H) ppm; ^{13}C NMR (75 MHz, CD_3OD): 180.47, 161.14, 146.04, 134.13, 130.89, 80.24, 44.14, 41.98, 28.81, 24.21, 23.95, 16.54 ppm; HRMS-CI$^+$: calcd for $C_{26}H_{44}N_7O_2$: 486.356; *m/z*: found: 486.357.

1,3-(4,5-Dihydro-1*H*-imidazol-2-yl)aminomethyl-5-bis(aminomethyl)-2,4,6-triethylbenzene (19): Trifluoroacetic acid (10 mL) was added to a solution of **18** (0.27 g, 0.44 mmol) in water, and the reaction mixture was allowed to stir for 2 h. The solvent was removed, and the anions were exchanged with an anion-exchange resin to acetates. The water solution was then lyophilized to yield a white solid (0.25 g, 100%). M.p. 250 °C (decomp); ^{1}H NMR (300 MHz, CD_3OD): δ = 4.43 (s, 4H), 4.20 (s, 2H), 3.76 (s, 8H), 2.78 (q, 6H), 1.83 (s, 9H), 1.20 (t, 9H) ppm; ^{13}C NMR (75 MHz, CD_3OD): δ = 179.04, 160.07, 145.27, 130.43, 63.16, 43.01, 40.80, 22.98, 15.31 ppm; HRMS-CI$^+$: *m/z*: calcd for $C_{18}H_{32}N_5$: 386.303; found: 386.304.

1,3-Bis[[(1,1-dimethylethoxy)carbonyl]aminomethyl]-5-(4,5-dihydro-*N*-(1,1-dimethylethoxy)carbonyl-imidazol-2-yl)aminomethyl-2,4,6-triethylbenzene (20): *N*-(1,1-Dimethylethoxycarbonyl)-2-methylthio-2-imidazoline (0.72 g, 3.3 mmol) was added to a solution of **16** (1.10 g, 2.5 mmol) in ethanol (20 mL) and glacial acetic acid (2.5 mL). The mixture was heated to 60 °C for 10 h, and then allowed to cool to room temperature over an additional 10 h. After removal of the solvent, the mixture was purified by column chromatography (silica gel, 1–4% ammonia sat. methanol in dichloromethane). An impurity was still present with the compound, so recrystallization was performed with dichloromethane (0.77 g, 51%). M.p. 165–167 °C; ^{1}H NMR (300 MHz, $CDCl_3$): δ = 6.70 (brs, 1H), 4.44 (s, 2H), 4.40 (brs, 2H), 4.32 (s, 4H), 3.84 (m, 4H), 2.70 (q, 6H), 1.43 (s, 27H), 1.17 (t, 9H) ppm; ^{13}C NMR (75 MHz, $CDCl_3$): δ = 155.64, 153.9, 153.3, 144.2, 132.54, 82.80, 48.19, 46.93, 41.37, 39.01, 28.41, 23.21, 16.74 ppm; HRMS-CI$^+$: *m/z*: calcd for $C_{33}H_{56}N_5O_6$: 618.423; found: 618.423.

1-(4,5-Dihydro-1*H*-imidazol-2-yl)aminomethyl-3,5-bis(aminomethyl)-2,4,6-triethylbenzene (21): Trifluoroacetic acid (15 mL) was added to a solution of **20** (0.767 g, 1.24 mmol) in dichloromethane, and the solution was allowed to stir for 2 h. The solvent was removed, and the anions were exchanged with an anion-exchange resin to acetates. The aqueous solution was then lyophilized to yield a white solid (0.610 g, 98%). M.p. 250 °C (decomp); ^{1}H NMR (300 MHz, CD_3OD): δ = 4.46 (s, 2H), 4.26 (s, 4H), 3.78 (s, 4H), 2.80 (q, 6H), 1.84 (s, 9H), 1.21 (t, 9H) ppm; ^{13}C NMR (75 MHz, $CDCl_3$): δ = 180.20, 161.42, 147.14, 146.63, 131.83, 130.58, 44.16, 41.86, 37.69, 24.28, 24.12, 16.40 ppm; HRMS-CI$^+$: *m/z*: calcd for $C_{18}H_{32}N_5$: 318.266; found: 318.266.

X-ray crystal structure determination of $C_{16}H_{20}BNO_2$ (14): Crystals grew as large colorless prisms by crystallization from methanol. The data crystal was cut from a much larger crystal and had approximate dimensions of 0.1 × 0.1 × 0.1 mm. The data were collected on a Nonius Kappa CCD diffractometer with a graphite monochromator with $Mo_{K\alpha}$ radiation (λ = 0.71073 Å). A total of 298 frames of data were collected by use of ω scans with a scan range of 1° and a counting time of 51 seconds per frame. The data were collected at 153 K with an Oxford Cryostream low-temperature device. Details of crystal data, data collection, and structure refinement are listed in Table 1 of the CCDC data. Data reduction was performed with DENZO-SMN.[57] The structure was solved by direct methods with SIR92[58] and refined by full-matrix, least-squares on F^2 with anisotropic displacement parameters for the non-H atoms with SHELXL-97.[59] The hydrogen atoms on carbon were calculated in ideal positions with isotropic displacement parameters set to 1.2 × U_{eq} of the attached atom (1.5 × U_{eq} for methyl hydrogen atoms). The hydrogen atom bound to the nitrogen atom was found in a ΔF map and refined with an isotropic displacement parameter. The function $\Sigma w(|F_o|^2 - |F_c|^2)^2$ was minimized, where $w = 1/[(\sigma(F_o))^2 + (0.0537P)^2 + (0.4446P)]$ and $P = (|F_o|^2 + 2|F_c|^2)/3$. $R_w(F^2)$ refined to 0.119, with $R(F)$ equal to 0.0446 and a goodness of fit (S) = 1.01. Definitions used for calculation of $R(F)$, $R_w(F^2)$, and the goodness of fit (S) are given below.[60] The data were corrected for secondary extinction effects. The correction takes the form: $F_{corr} = kF_c/[1 + (1.7(4) \times 10^{-5}) \times F_c^2\lambda^3/(\sin 2\theta)]^{0.25}$, where k is the overall scale factor. Neutral atom scattering factors and values used to calculate the linear absorption coefficient are from the International Tables for X-ray Crystallography.[61] All figures were generated by use of SHELXTL/PC.[59] Tables of positional and thermal parameters, bond lengths and angles, torsion angles, figures and lists of observed and calculated structure factors are located in the CCDC data.

CCDC-232031 contains the supplementary crystallographic data for this paper. These data can be obtained free of charge via www.ccdc.cam.ac.uk/conts/retrieving.html, or from the Cambridge Crystallographic Data Centre, 12 Union Road, Cambridge CB2 1EZ, UK; fax: (+44)1223–336033; or email: deposit@ccdc.cam.ac.uk.

Acknowledgment

We gratefully acknowledge support for this project from the Texas Advanced Technology Program, the National Institutes of Health GM57306, the Beckman Center for Arrayed Sensors, and the Welch Foundation.

[1] a) M. M. G. Antonisse, D. N. Reinhoudt, *Chem. Commun.* **1998**, 443–448; b) P. D. Beer, P. A. Gale, *Angew. Chem.* **2001**, *113*, 502–532; *Angew. Chem. Int. Ed.* **2001**, *40*, 486–516; c) B. Linton, A. D. Hamilton, *Chem. Rev.* **1997**, *97*, 1669–1680; d) R. Reichenback-Klinke, B. Konig, *J. Chem. Soc. Dalton Trans.* **2002**, 121–130; e) J. K. M. Sanders, *Pure Appl. Chem.* **2000**, *72*, 2265–2274; f) F. P. Schmidtchen, M. Berger, *Chem. Rev.* **1997**, *97*, 1609–1646; g) H.-J. Schneider, *Angew. Chem.* **1991**, *103*, 1419–1439; *Angew. Chem. Int. Ed. Engl.* **1991**, *30*, 1417–1436; h) T. S. Snowden, E. V. Anslyn, *Curr. Opin. Chem. Biol.* **1999**, *3*, 740–746.

[2] a) M. Inouye, T. Miyake, M. Furusyo, H. Nakazumi, *J. Am. Chem. Soc.* **1995**, *117*, 12416–12425; b) M. Inouye, J. Chiba, H. Nakazumi, *J. Org. Chem.* **1999**, *64*, 8170–8176.

[3] P. T. Lewis, C. J. Davis, L. A. Cabell, M. He, M. W. Read, M. E. McCarroll, R. M. Strongin, *Org. Lett.* **2000**, *2*, 589–592.

[4] a) R. Breslow, B. Zhang, *J. Am. Chem. Soc.* **1996**, *118*, 8495–8496; b) T. W. Bell, Z. Hou, Y. Luo, M. G. B. Drew, E. Chapoteau, B. P. Czech, A. Kumar, *Science* **1995**, *269*, 671–674; c) T. W. Bell, Z. Hou, *Angew. Chem.* **1997**, *109*, 1601–1603; *Angew. Chem. Int. Ed. Engl.*

1997, *36*, 1536–1538; d) S. C. Zimmerman, Z. Zeng, *J. Org. Chem.* **1990**, *55*, 4789–4791.
[5] a) F. Unob, Z. Asfari, J. Vicens, *Tetrahedron Lett.* **1998**, *39*, 2951–2954; b) T. Hirano, K. Kikuchi, Y. Urano, T. Higuchi, T. Nagano, *J. Am. Chem. Soc.* **2000**, *122*, 12399–12400; c) T. W. Bell, P. J. Cragg, A. Firestone, A. D. I. Kwok, J. Liu, R. Ludwig, A. Sodoma, *J. Org. Chem.* **1998**, *63*, 2232–2243.
[6] a) J. Chin, C. Walsdorff, B. Stranix, J. Oh, H. J. Chung, S.-M. Park, K. Kim, *Angew. Chem.* **1999**, *111*, 2923–2926; *Angew. Chem. Int. Ed.* **1999**, *38*, 2756–2759; b) A. P. Davis, J. F. Gilmer, J. J. Perry, *Angew. Chem.* **1996**, *108*, 1410–1413; *Angew. Chem. Int. Ed. Engl.* **1996**, *35*, 1312–1315; c) V. Amendola, E. Bastianello, L. Fabbrizzi, C. Mangano, P. Pallavicini, A. Perotti, A. M. Lanfredi, F. Ugozzoli, *Angew. Chem.* **2000**, *112*, 3039–3042; *Angew. Chem. Int. Ed.* **2000**, *39*, 2917–2920.
[7] L. Sebo, B. Schweizer, F. Diederich, *Helv. Chim. Acta* **2000**, *83*, 80–92.
[8] a) J. M. Lehn, *J. Inclusion Phenom.* **1988**, *6*, 351–396; b) D. J. Cram, *Science* **1983**, *219*, 1177–1183; c) D. J. Cram, *Science* **1988**, *240*, 760–767; d) C. J. Pedersen, *Science* **1988**, *241*, 536–540.
[9] B. Linton, A. D. Hamilton, *Tetrahedron* **1999**, *55*, 6027–6038.
[10] K. Niikura, A. Metzger, E. V. Anslyn, *J. Am. Chem. Soc.* **1998**, *120*, 8533–8534.
[11] R. J. Fitzmaurice, G. M. Kyne, D. Douheret, J. D. Kilburn, *J. Chem. Soc. Perkin Trans. 1* **2002**, 841–864.
[12] B. Dietrich, D. L. Fyles, T. M. Fyles, J. M. Lehn, *Helv. Chim. Acta* **1979**, *62*, 2763–2787.
[13] C. L. Hannon, E. V. Anslyn, *Bioorg. Chem. Front* **1993**, *3*, 193–255.
[14] a) M. Berger, F. P. Schmidtchen, *J. Am. Chem. Soc.* **1999**, *121*, 9986–9993; b) M. Berger, F. P. Schmidtchen, *Angew. Chem.* **1998**, *110*, 2840–2842; *Angew. Chem. Int. Ed.* **1998**, *37*, 2694–2696; c) A. Metzger, K. Gloe, H. Stephan, F. P. Schmidtchen, *J. Org. Chem.* **1996**, *61*, 2051–2055; d) P. Schiessl, F. P. Schmidtchen, *Tetrahedron Lett.* **1993**, *34*, 2449–2452.
[15] M. Haj-Zaroubi, N. W. Mitzel, F. P. Schmidtchen, *Angew. Chem.* **2002**, *114*, 111–114; *Angew. Chem. Int. Ed.* **2002**, *41*, 104–107.
[16] a) B. R. Linton, M. S. Goodman, E. Fan, S. A. van Arman, A. D. Hamilton, *J. Org. Chem.* **2001**, *66*, 7313–7319; b) A. P. Sukharevsky, I. Read, B. Linton, A. D. Hamilton, D. H. Waldeck, *J. Phys. Chem. B* **1998**, *102*, 5394–5403.
[17] A. P. Davis, R. S. Wareham, *Angew. Chem.* **1999**, *111*, 3160–3179; *Angew. Chem. Int. Ed.* **1999**, *38*, 2978–2996.
[18] a) J. Bitta, S. Kubik, *Org. Lett.* **2001**, *3*, 2637–2640; b) T. K. Chakraborty, S. Tapadar, S. Kiran Kumar, *Tetrahedron Lett.* **2002**, *43*, 1317–1320.
[19] T. Fujimoto, C. Shimizu, O. Hayashida, Y. Aoyama, *J. Am. Chem. Soc.* **1997**, *119*, 6676–6677.
[20] R. D. Hubbard, S. R. Horner, B. L. Miller, *J. Am. Chem. Soc.* **2001**, *123*, 5810–5811.
[21] V. Kral, O. Rusin, F. P. Schmidtchen, *Org. Lett.* **2001**, *3*, 873–876.
[22] J. P. Lorand, J. O. Edwards, *J. Org. Chem.* **1959**, *24*, 769–774.
[23] a) J. C. Norrild, H. Eggert, *J. Chem. Soc. Perkin Trans. 2* **1996**, 2583–2588; b) J. Yoon, A. W. Czarnik, *J. Am. Chem. Soc.* **1992**, *114*, 5874–5875; c) K. R. A. Sandanayake, S. Shinkai, *J. Chem. Soc. Chem. Commun.* **1994**, 1083–1084; d) M. J. Deetz, B. D. Smith, *Tetrahedron Lett.* **1998**, *39*, 6841–6844; e) C. J. Ward, P. R. Ashton, T. D. James, P. Patel, *Chem. Commun.* **2000**, 229–230; f) G. Springsteen, B. Wang, *Chem. Commun.* **2001**, 1608–1609.
[24] G. Wulff, *Pure Appl. Chem.* **1982**, *54*, 2093–2102.
[25] T. D. James, K. R. A. S. Sandanayake, S. Shinkai, *J. Chem. Soc. Chem. Commun.* **1994**, 477–478.
[26] T. D. James, K. R. A. S. Sandanayake, R. Iguchi, R. S. Shinkai, *J. Am. Chem. Soc.* **1995**, *117*, 8982–8987.
[27] a) G. Springsteen, B. Wang, *Tetrahedron* **2002**, *58*, 5291–5300.
[28] J. M. Conner, V. C. Bulgrin, *J. Inorg. Nucl. Chem.* **1967**, *29*, 1953–1961.
[29] H.-D. Belita, W. Grosch, *Food Chemistry*, Springer, Berlin, Heidelberg, **1999**.
[30] M. R. Bronze, L. F. Vilas Boas, A. P. Belchior, *J. Chromatogr. A* **1997**, *768*, 143–152; D. M. Goldberg, B. Hoffman, J. Yang, G. J. Soleas, *J. Agric. Food Chem.* **1999**, *47*, 3978–3985.
[31] L. K. Ng, P. Lafontaine, J. Harnois, *J. Chromatogr. A* **2000**, *873*, 29–38.
[32] a) D. J. Iverson, G. Hunter, J. F. Blount, J. R. Damewood, Jr., K. Mislow, *J. Am. Chem. Soc.* **1981**, *103*, 6073–6083; b) K. V. Kilway, J. S. Siegel, *J. Am. Chem. Soc.* **1992**, *114*, 255–261; c) H.-W. Marx, F. Moulines, T. Wagner, D. Astruc, *Angew. Chem.* **1996**, *108*, 1842–1845; *Angew. Chem. Int. Ed. Engl.* **1996**, *35*, 1701–1704; d) T. D. P. Stack, Z. Hou, K. N. Raymond, *J. Am. Chem. Soc.* **1993**, *115*, 6466–6467.
[33] A. Metzger, V. M. Lynch, E. V. Anslyn, *Angew. Chem.* **1997**, *109*, 911–914; *Angew. Chem. Int. Ed. Engl.* **1997**, *36*, 862–865.
[34] A. Metzger, E. V. Anslyn, *Angew. Chem.* **1998**, *110*, 682–684; *Angew. Chem. Int. Ed.* **1998**, *37*, 649–652.
[35] S. L. Wiskur, H. Ait-Haddou, J. J. Lavigne, E. V. Anslyn, *Acc. Chem. Res.* **2001**, *34*, 963–972.
[36] M. J. Perry, in *Monoclonal Antibodies: Principles and Applications* (Eds.: J. R. Birch, E. S. Lennox), Wiley–Liss, New York, **1995**, pp. 107–120.
[37] J. J. Lavigne, E. V. Anslyn, *Angew. Chem.* **1999**, *111*, 3903–3906; *Angew. Chem. Int. Ed.* **1999**, *38*, 3666–3669.
[38] S. L. Wiskur, E. V. Anslyn, *J. Am. Chem. Soc.* **2001**, *123*, 10109–10110.
[39] R. E. Hanes, Jr., J. J. Lavigne, E. V. Anslyn, K. V. Kilway, J. Seigel, unpublished results.
[40] S. R. Mundla, L. J. Wilson, S. R. Klopfenstein, W. L. Seibel, N. N. Nikolaides, *Tetrahedron Lett.* **2000**, *41*, 6563–6566.
[41] a) K. N. Koh, K. Araki, A. Ikeda, H. Otsuka, S. Shinkai, *J. Am. Chem. Soc.* **1996**, *118*, 755–758; b) M. Inouye, K-I. Hashimoto, K. Isagawa, *J. Am. Chem. Soc.* **1994**, *116*, 5517–5518.
[42] K. A. Connors, *Binding Constants, The Measurement of Molecular Stability*, Wiley, New York, **1987**.
[43] a) D. E. Hughes, M. J. Cardone, *Anal. Chem.* **1980**, *52*, 940–942; b) H. B. Corbin, *Anal. Chem.* **1973**, *45*, 534–537.
[44] a) S. Friedman, B. Pace, R. Pizer, *J. Am. Chem. Soc.* **1974**, *96*, 5381–5384; b) L. I. Katzin, E. Gulyas, *J. Am. Chem. Soc.* **1966**, *88*, 5209–5212; c) K. Kustin, R. Pizer, *J. Am. Chem. Soc.* **1969**, *91*, 317–322.
[45] C. W. Gray, Jr., T. A. Houston, *J. Org. Chem.* **2002**, *67*, 5426–5428.
[46] T. Mancilla, R. Contreras, B. Wrackmeyer, *J. Organomet. Chem.* **1986**, *307*, 1–6.
[47] L. K. Mohler, A. W. Czarnik, *J. Am. Chem. Soc.* **1993**, *115*, 7037–7038.
[48] S. Friedman, R. Pizer, *J. Am. Chem. Soc.* **1975**, *97*, 6059–6062.
[49] S. L. Wiskur, J. J. Lavigne, H. Ait-Haddou, V. Lynch, Y. H. Chiu, J. W. Canary, E. V. Anslyn, *Org. Lett.* **2001**, *3*, 1311–1314.
[50] C. R. Cooper, T. D. James, *Chem. Lett.* **1998**, 883–884.
[51] R. A. Bissell, A. Prasanna de Silva, H. Q. N. Gunaratne, P. L. M. Lynch, G. E. M. Maguire, C. P. McCoy, K. R. A. S. Sandanayake, *Top. Curr. Chem.* **1993**, *168*, 223–264.
[52] M. Stoedeman, I. Wadsoe, *Pure Appl. Chem.* **1995**, *67*, 1059–1068; I. Wadsoe, *Chem. Soc. Rev.* **1997**, *26*, 79–86.
[53] M. Rekharsky, Y. Inoue, S. L. Tobey, A. Metzger, E. V. Anslyn, *J. Am. Chem. Soc.* **2002**, *124*, 14959–14967.
[54] S. Sun, M. A. Fazal, B. C. Roy, B. Chandra, S. Mallik, *Inorg. Chem.* **2002**, *41*, 1584–1590.
[55] W. P. Jencks, *Proc. Natl. Acad. Sci. USA* **1981**, *78*, 4046–4050.
[56] D. A. Bell, S. G. Diaz, S. G, V. M. Lynch, E. V. Anslyn, *Tetrahedron Lett.* **1995**, *36*, 4155–4158.
[57] Z. Otwinowski, W. Minor, *Methods Enzymol.* **1997**, *276*, 307–326.
[58] A. Altomare, G. Cascarano, C. Giacovazzo, A. Guagliardi, *J. Appl. Crystallogr.* **1993**, *26*, 343–350.
[59] G. M. Sheldrick, 5.03 ed., Siemens Analytical X-Ray Instruments, Madison, Wisconsin, **1994**.
[60] $Rw(F^2) = \{w(|F_o|^2 - |F_c|^2)^2/w(|F_o|)^4\}^{1/2}$ where w is the weight given each reflection. $R(F) = (|F_o| - |F_c|)/|F_o|\}$ for reflections with $F_o > 4((F_o))$. $S = [w(|F_o|^2 - |F_c|^2)^2/(n-p)]^{1/2}$, where n is the number of reflections and p is the number of refined parameters.
[61] *International Tables for X-ray Crystallography*, *Vol. C*, Kluwer Academic Press, Boston, **1992** .

Received: November 20, 2003
Revised: March 4, 2004
Published online: June 21, 2004

